View metadata, citation and similar papers at core.ac.uk

brought to you by CORE

provided by Depositum

soil systems

MDPI

Article

Organo-Mineral Interactions Are More Important for Organic Matter Retention in Subsoil Than Topsoil

Vincent Poirier [1,*], Isabelle Basile-Doelsch [2], Jérôme Balesdent [2], Daniel Borschneck [2], Joann K. Whalen [3] and Denis A. Angers [4]

[1] Unité de Recherche et Développement en Agriculture et Agroalimentaire de l'Abitibi-Témiscamingue, Université du Québec en Abitibi-Témiscamingue, 79 rue Côté, Notre-Dame-du-Nord, Québec, J0Z 3B0, Canada

[2] Aix-Marseille Université, CNRS, IRD, INRA, Collège de France, CEREGE, Europôle Méditerranéen de l'Arbois, BP 80, 13545 Aix-en-Provence, France; basile@cerege.fr (I.B.-D.); jerome.balesdent@inra.fr (J.B.); borschneck@cerege.fr (D.B.)

[3] Department of Natural Resource Sciences, Macdonald Campus of McGill University, 21111 Lakeshore Road, Ste-Anne-de-Bellevue, Québec, H9X 3V9, Canada; joann.whalen@mcgill.ca

[4] Quebec Research and Development Centre, Agriculture and Agri-Food Canada, 2560 Hochelaga Blvd., Québec, Québec, G1V 2J3C, Canada; denis.angers@canada.ca

* Correspondence: vincent.poirier@uqat.ca; Tel.: +1-819-762-0971 (ext. 5912)

Received: 30 September 2019; Accepted: 20 December 2019; Published: 7 January 2020

Abstract: Decomposing crop residues contribute to soil organic matter (SOM) accrual; however, the factors driving the fate of carbon (C) and nitrogen (N) in soil fractions is still largely unknown, especially the influence of soil mineralogy and autochthonous organic matter concentration. The objectives of this work were (1) to evaluate the retention of C and N from crop residue in the form of occluded and mineral-associated SOM in topsoil (0–20 cm) and subsoil (30–70 cm) previously incubated for 51 days with ^{13}C-^{15}N-labelled corn residues, and (2) to explore if specific minerals preferentially control the retention of residue-derived C and N in topsoil and subsoil. We used topsoil and subsoil having similar texture and mineralogy as proxies for soils being rich (i.e., topsoil) and poor (i.e., subsoil) in autochthonous organic matter. We performed a sequential density fractionation procedure and measured residue-derived C and N in occluded and mineral-associated SOM fractions, and used X-ray diffraction analysis of soil density fractions to investigate their mineralogy. In accordance with our hypothesis, the retention of C and N from crop residue through organo-mineral interactions was greater in subsoil than topsoil. The same minerals were involved in the retention of residue-derived organic matter in topsoil and subsoil, but the residue-derived organic matter was associated with a denser fraction in the subsoil (i.e., 2.5–2.6. g cm^{-3}) than in the topsoil (i.e., 2.3–2.5 g cm^{-3}). In soils and soil horizons with high clay content and reactive minerals, we find that a low SOM concentration leads to the rapid stabilization of C and N from newly added crop residues.

Keywords: soil organic matter; crop residue; topsoil; subsoil; soil mineralogy; mineral-associated soil organic matter

1. Introduction

Soil organic matter (SOM), the largest terrestrial carbon (C) pool and the main nitrogen (N) source for plant growth, accumulates during plant residue decomposition and has the potential to improve soil fertility and mitigate climate change [1–3]. SOM accumulates through two mechanisms—occlusion within soil aggregates and association with mineral surfaces [4–6]. Occluded SOM is enriched with C-

rich, plant-like compounds and persists for decades, whereas mineral-associated SOM is enriched with N-rich, microbially processed compounds with a residence time of centuries [7–9]. Two key soil parameters determine whether plant residue will be occluded or transformed into mineral-associated SOM, namely soil mineralogy and the amount of organic matter initially in the soil (i.e., autochthonous organic matter).

Organic compounds adsorb to the reactive surfaces of soil minerals and are protected against biodegradation through organo-mineral interactions [5,6]. Soils with higher clay content and reactive minerals (i.e., illite + chlorite, montmorillonite, vermiculite, and amorphous minerals [10,11]) are expected to have a high specific surface area for adsorption of organic matter. Such soils have a high capacity to retain C and N from crop residue as mineral-associated SOM [12,13]. The mineral-associated SOM fraction in these soils is often quantified using the density-based separation method, since mineral-associated SOM occurs in denser fractions of the soil (i.e., ρ >1.9 g cm^{-3}) [4,9,14,15]. However, quantifying the SOM associated with each type of reactive mineral present in soil is more complex. Sequential separation of the soil using predefined density thresholds is a way to partition the mineral-associated fraction into subfractions with specific mineralogy [14,16,17]. This approach can distinguish SOM bound to different soil minerals within the mineral-associated fraction.

The concentration of autochthonous organic matter also affects the amount of residue-derived C and N retained in mineral-associated SOM. For a given mineralogy, soils with a low SOM concentration contain more reactive mineral surfaces that are not occupied by autochthonous organic matter, and could retain more C and N from crop residue on mineral surfaces than soil with a high SOM concentration [18,19]. The effect of autochthonous organic matter on residue-derived C and N retention can be tested using topsoil (i.e., 0–20 cm depth) and subsoil (i.e., >20 cm depth) from the same profile, which should have similar texture and mineralogy and the same historical agricultural practices [19–21]. We expect the SOM-poor subsoil to retain more C and N from crop residue on mineral surfaces than the SOM-rich topsoil [22,23]. In the fine-textured soils of Eastern Canada, the subsoil contains about five times less autochthonous organic C and total N than the topsoil, suggesting a greater capacity for residue-derived C and N retention through organo-mineral interactions in the subsoil [13,18,21].

The objective of this work was to evaluate the retention of C and N from crop residue in the occluded and mineral-associated SOM pools of topsoil and subsoil after 51 d of incubation with ^{13}C-^{15}N-labelled corn residues [21]. We hypothesized that more residue-derived C and N would be retained in the mineral-associated SOM fraction of subsoil than topsoil. A secondary objective of this work was to determine if specific soil minerals bind preferentially to C and N from crop residue in topsoil and subsoil.

2. Materials and Methods

2.1. Soils and Incubation

Topsoil (0–20 cm depth) and subsoil (30–70 cm depth) were collected in fall 2007 from a heavy clay soil from the Kamouraska series under a barley crop (*Hordeum vulgare* L.) in Lévis, Québec, Canada (46°48′ N, 71°23′ W). The soil is considered a Haplic Gleysol according to the World Reference Base for Soil Resources system [24] and an Orthic Humic Gleysol according to the Canadian System of Soil Classification [25]. The topsoil and subsoil had similar texture and mineralogy, that is, they contained 276 g kg^{-1} of silt (2–50 μm) and 665 g kg^{-1} of clay (<2 μm) with quartz, albite, microcline, amphibole, chlorite, vermiculite, and illite/muscovite as major minerals. Soil pH (1:2 soil-to-$CaCl_2$ 0.01 M ratio) was 5.2 in topsoil and 6.3 in subsoil. There was no inorganic C in topsoil and subsoil; soil organic C concentration was therefore equivalent to the total C concentration.

Samples for this study were topsoil and subsoil incubated for 51 d under aerobic conditions with (10 g C kg^{-1} soil) or without (0 g C kg^{-1} soil) labelled corn residues. Briefly, 150 g of 6 mm sieved, air-dried topsoil and subsoil were placed in separate 1 L glass jars with 0 (control) and 3.45 g (equivalent to 10 g residue C kg^{-1} soil) of ^{13}C-^{15}N-labelled residues. The residue, from young corn shoots (*Zea mays* L. cv.

Cargill 2610-L), contained 434 g C kg^{-1} and 16 g N kg^{-1}, had a ^{13}C isotopic signature ($\delta^{13}C$) of 69.7‰ and an atom% ^{15}N (At%^{15}N) of 7.4%, and a particle size of 0.1 mm to 1 mm. Soil-residue mixtures were moistened to −38 kPa and incubated at 25 °C for 51 d. For residue-amended soils, the soil-residue mixture was adjusted to a C/N ratio of 10 with KNO_3. See Poirier et al. [21] for further details on incubation conditions.

2.2. Sequential Density Separation

Density thresholds were based on theoretical densities of organo-mineral complexes for major soil minerals, considering the mineral density and an arbitrary SOC concentration determined from the mineral's capacity to adsorb SOM (using mineral specific surface area as a proxy). The detailed calculation procedure is presented in Appendix A. According to the density thresholds of ϱ = 1.9, 2.1, 2.3, 2.5, and 2.6 g cm^{-3} (hereafter, density thresholds are reported without stating g cm^{-3}) we prepared density separation solutions using LST Fastfloat (80% sodium heteropolytungstate) [26]. Since undiluted LST is acidic (pH < 4.0), we added 0.14 ± 0.01 g NaOH g^{-1} undiluted LST to increase the pH of density solutions to 6.6 ± 0.3.

Whole soil was separated into seven fractions. The first step separated the non-occluded light fraction (NOLF) (ρ < 1.9). Air-dried soil (7.5 g) was weighed in a 30 mL polycarbonate Nalgene® Oak Ridge centrifuge tube (Thermo Fischer Scientific Inc., Waltham, MA, USA). After adding 20 mL of ρ = 1.9 LST, the contents were manually shaken end-to-end 20 times, allowed to settle overnight, then centrifuged at 12,500 × *g* for 10 to 26 min. Centrifugation time was determined according to Stokes's law based on (1) the particle size threshold of 0.2 μm, (2) the difference between the density of the solution and the mineral particles, and (3) the viscosity of LST solutions [26]. Soil particles <0.2 μm and dissolved organic matter were not recovered. The supernatant containing NOLF (ρ < 1.9) was siphoned from the tube, rinsed three times with 25 mL deionized water, and recovered by centrifugation, then freeze-dried prior to subsequent analysis.

The second step retrieved the occluded light fraction (OLF) (ρ < 1.9) by re-suspending the soil pellet with 18 mL of ρ = 1.9 LST solution and dispersing it by sonication in an ice bath. The soil solution was first pulse sonicated (5.5 s on, 9.9 s off) for 30 s at 70% energy input (i.e., short duration, high energy) and then pulse sonicated (9.9 s on, 2.5 s off) for 4 min at 35% energy input (i.e., long duration, low energy). Next, the soil solution was centrifuged (128 min) at 12,500 × *g*, the supernatant was siphoned, a second 18 mL aliquot of ρ = 1.9 LST solution was added, and the long duration, low energy sonication was repeated before centrifuging and siphoning the supernatant. Total energy input to the soil solution during OLF separation was 520 J ml^{-1}. The combined OLF was diluted with 980 mL deionized water and concentrated by multiple centrifugations (26 min each). The OLF was rinsed in 25 mL deionized water, pulse sonicated (short duration, high energy), and centrifuged (10 min). The rinsing step was repeated three times, resulting in a total energy input of 125 J ml^{-1}, then freeze-dried before analysis.

The five subsequent steps isolated five density fractions (ρ = 1.9–2.1, 2.1–2.3, 2.3–2.5, 2.5–2.6, and >2.6) from the soil pellet. Each time, the remaining soil was re-suspended with 15 to 25 mL of the required LST solution. The soil–LST mixture was pulse sonicated (short duration, high energy) and centrifuged and the supernatant siphoned. Centrifugation times were 134, 150, 210, and 270 min for 1.9–2.1, 2.1–2.3, 2.3–2.5, and 2.5–2.6 fractions, respectively. However, prolonged centrifugation for 510 min occurred during the second separation of the 2.3–2.5 fraction since no distinct phases were observed after 210 min. Total energy input to the soil solution during density fraction separation was 230 J ml^{-1}. For each fraction, the density separation occurred twice and all supernatant was combined, diluted with 100 to 300 mL deionized water, and re-concentrated by multiple centrifugations (10 min each). Density fractions were rinsed three times, recovered by centrifugation and freeze-dried prior to analysis. Figure 1 illustrates how methodological fractions relate to functional fractions of SOM.

2.3. Mineralogical Analysis

Soil mineralogy was determined on randomly oriented powders with an X-ray diffractometer (X'Pert Pro MPD, PANalytical, Limeil-Brévannes, France) running at 40 kV and 40 mA using Co-Kα radiation (λ = 1.79 Å) with a linear detector X'Celerator and a secondary flat monochromator. Samples of whole soil and soil density fractions were crushed in an agate mortar, put in cylindrical aluminum holders, and spun at 15 rpm. A counting time of 3 s per 0.033° step was used for 2θ in the 3.5° to 80.0° range. The X'Pert High Score 3.0 software (Almelo, Netherlands) [27] was used to identify minerals.

2.4. Carbon and Nitrogen Analyses

Soil organic C (SOC) and total soil N concentrations, $\delta^{13}C$ and At%^{15}N in density fractions, were measured using an elemental analyzer (Carlo Erba NA 1500, CE Instruments, Rodano, Italy) coupled with an isotopic ratio mass spectrometer (Thermo-Finnigan, Delta S, Bremen, Germany). The $\delta^{13}C$ (in ‰) was calculated as follows:

$$\delta^{13}C = [(^{13}R_{sample} - {}^{13}R_{standard})/{}^{13}R_{standard}] \times 1000, \quad (1)$$

where $^{13}R = {}^{13}C/{}^{12}C$ and the standard is the international Vienna Pee Dee Belemnite. The At%^{15}N (in %) was calculated according to the following:

$$At\%^{15}N = [\text{no. of } {}^{15}N \text{ atoms}/(\text{no. of } ({}^{15}N + {}^{14}N) \text{ atoms})] \times 100. \quad (2)$$

The fraction of total SOC coming from residue C (f_C, in g residue C g^{-1} total SOC) and total soil N coming from residue N (f_N, in g residue N g^{-1} total soil N) was calculated as follows:

$$f_C \text{ or } f_N = [(\delta_{TR} \text{ or } At_{TR}) - (\delta_C \text{ or } At_C)]/[(\delta_R \text{ or } At_R) - (\delta_C \text{ or } At_C)], \quad (3)$$

where δ_{TR} and At_{TR} represent $\delta^{13}C$ and At%^{15}N of the soil receiving residue, δ_C and At_C represent $\delta^{13}C$ and At%^{15}N of the control soil (no residue), and δ_R and At_R represent $\delta^{13}C$ and At%^{15}N of the corn residue, respectively. Residue C and N concentrations in soil (in g residue C or N kg^{-1} soil) were as follows:

$$\text{residue C or N} = f_{C \text{ or }} f_N \times \text{SOC or SN}, \quad (4)$$

where SOC and SN are the concentrations of total soil organic C (g SOC kg^{-1} soil) and total soil N (g total soil N kg^{-1} soil), respectively.

2.5. Relationships between Methodological and Functional Fractions of SOM

We assumed that SOM retained in the soil matrix was present in OLF and ρ >1.9 fractions. Soil organic C retained by the soil matrix (SOC_R, in g SOC kg^{-1} soil) was as follows:

$$SOC_R = SOC_{OLF} + SOC_{1.9–2.1} + SOC_{2.1–2.3} + SOC_{2.3–2.5} + SOC_{2.5–2.6} + SOC_{>2.6}, \quad (5)$$

where $SOC_{OLF \text{ to } >2.6}$ is the SOC concentration in each density fraction (in g SOC kg^{-1} soil). Total soil N_R, residue C_R, and residue N_R were calculated similarly. Mineral-associated SOM was the sum of SOM in density fractions >1.9, expressed as the SOC_{MAOM}, in g SOC kg^{-1} soil as follows:

$$SOC_{MAOM} = SOC_{1.9–2.1} + SOC_{2.1–2.3} + SOC_{2.3–2.5} + SOC_{2.5–2.6} + SOC_{>2.6}. \quad (6)$$

Total soil N_{MAOM}, residue C_{MAOM}, and residue N_{MAOM} were calculated similarly. The mass of SOC occluded in the soil matrix ($SOC_{R\text{-}OLF}$, in g SOC_{OLF} 100 g^{-1} SOC_R) or in mineral-associated forms ($SOC_{R\text{-}MAOM}$, in g SOC_{MAOM} 100 g^{-1} SOC_R) was determined as follows:

$$SOC_{R\text{-}OLF \text{ or } R\text{-}MAOM} = (SOC_{OLF \text{ or } MAOM}/SOC_R) \times 100. \quad (7)$$

Total soil $N_{R\text{-}OLF \text{ and } R\text{-}MAOM}$, residue $C_{R\text{-}OLF \text{ and } R\text{-}MAOM}$, and residue $N_{R\text{-}OLF \text{ and } R\text{-}MAOM}$ were calculated similarly.

2.6. Statistical Analysis

The soil incubation experiment was a completely randomized factorial design with two soil horizons (topsoil and subsoil), two levels of residue (0 and 10 g C kg^{-1}), and three replicates of each treatment, for 12 experimental units incubated. Each of the 12 experimental soils was separated into seven density fractions (n = 84 fractions). The effect of soil horizons and residue inputs on occluded SOM and mineral-associated SOM fractions was evaluated by analysis of variance (ANOVA) with a linear mixed model using the MIXED procedure of SAS v. 9.3 (SAS Institute Inc., Cary, NC, USA) [28]. When residuals showed heterogeneity or non-normal distribution, data were log, square root, or ranked transformed. When differences were significant ($p < 0.05$), we used Fisher's least significant difference (LSD) test to separate treatment means. Graphical representations were done with SigmaPlot v. 13 (Systat Software Inc., San Jose, CA, USA) [29].

3. Results

3.1. Mass Distribution and Recovery

We recovered 881 ± 13 g kg^{-1} of soil particles after density separation, on average, across all soil horizons and residue treatments (n = 12), so only about 12% of the initial soil mass was lost during the procedure. In soil incubated without residue, most of the soil mass (~60%) was in the 2.3–2.5 fraction in topsoil and in the 2.5–2.6 fraction in subsoil (data not shown). Soil incubated with residue had significantly ($p < 0.002$) more OLF mass, resulting in as much as 39.5 g OLF kg^{-1} in topsoil with residue (1.2 times greater than in topsoil without residue) and 5.0 g OLF kg^{-1} in subsoil with residue (3.7-fold more than in subsoil without residue). Soil incubated with residue had less soil mass in the 2.3–2.5 fraction ($p < 0.03$) and a numerically greater soil mass of the 2.5–2.6 fraction of topsoil and subsoil (data not shown). Residue addition did not affect the mass of other fractions of the topsoil and subsoil.

3.2. Mineralogical Analysis of Soil Density Fractions

Residue addition did not influence the diffractograms of soil density fractions, so those of unamended soils are presented as an example (Figure 2). The soil matrix was dominated by primary minerals (quartz, albite, microcline, and muscovite), but secondary minerals (montmorillonite, chlorite, vermiculite, and illite) were observed in most density fractions. In topsoil (Figure 2a), the diffractograms of the fractions 1.9–2.1, 2.1–2.3, and 2.3–2.5 were similar; they showed broad peaks and diffusion bands at low angle, and small peaks of chlorite/vermiculite (at 7.3°), montmorillonite (at 8.4°) and illite/muscovite (at 10.3°). The intensity of chlorite (at 14.5°) and illite/muscovite (at 10.3°) peaks increased in the denser soil fractions, whereas the opposite was observed for montmorillonite (at 8.4°). The subsoil (Figure 2b) had a montmorillonite (at 8.4°) peak in the 2.3–2.5 fraction. Montmorillonite was also observed in lighter (<2.3) and heavier (>2.5) fractions. Larger peaks of montmorillonite (at 8.4°) and illite/muscovite (at 10.3°) were seen in the 2.1–2.3 and 2.3–2.5 fractions of subsoil than topsoil. In the 2.5–2.6 fraction, the diffusion band at low angle was clearly visible in subsoil and the intensity of the peaks of chlorite/vermiculite (at 7.3°), montmorillonite (at 8.4°) and illite/muscovite (at 10.3°) were greater in subsoil than in topsoil.

3.3. Residue C and N in Soil Density Fractions

Density fractions from subsoil had greater ($p < 0.004$) enrichment in residue C (f_C, Equation (3)) and residue N (f_N, Equation (3)) than density fractions from topsoil, except that the NOLF was less enriched in residue-N in subsoil than topsoil (Figure 3). Topsoil f_C values were similar among fractions with ρ >1.9 (Figure 3a). However, subsoil f_C values decreased with increasing density (Figure 3a), which was also the case for f_N values in both soils (Figure 3b). We recovered an average 76% of the residue-derived C in the density fractions and about 46% of the residue-derived N in the density fractions, in both soils (Table 1). Most of residue-derived C and N was in the NOLF (43% and 18%, respectively) and OLF (23% and 15%,

respectively; Table 1). Mineral-associated residue C and N accumulated preferentially in the 2.5–2.6 fraction of the subsoil and in the 2.3–2.5 fraction of topsoil (Table 1).

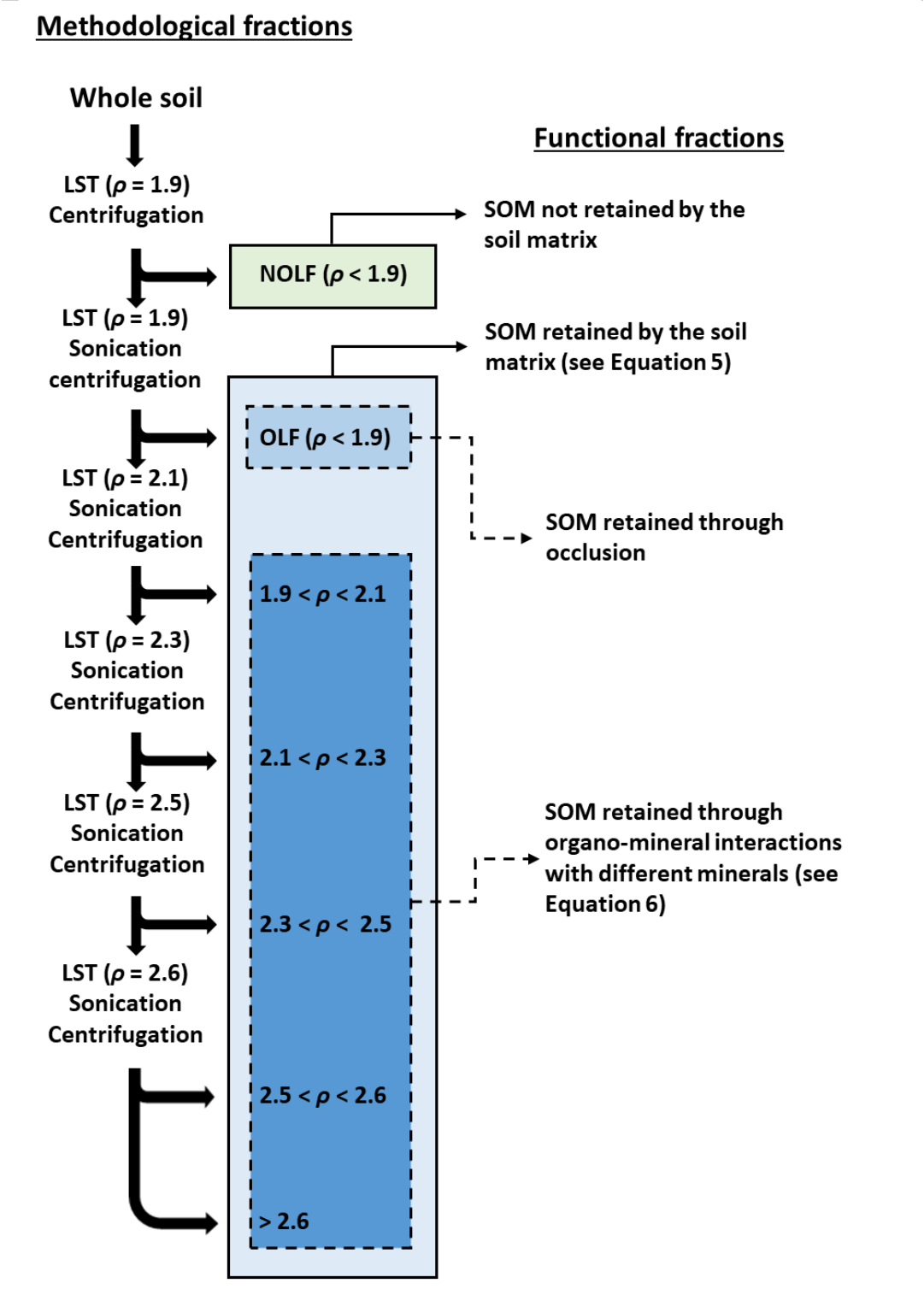

Figure 1. Fractionation scheme illustrating the methodological procedure and presumed functionality of soil organic matter.

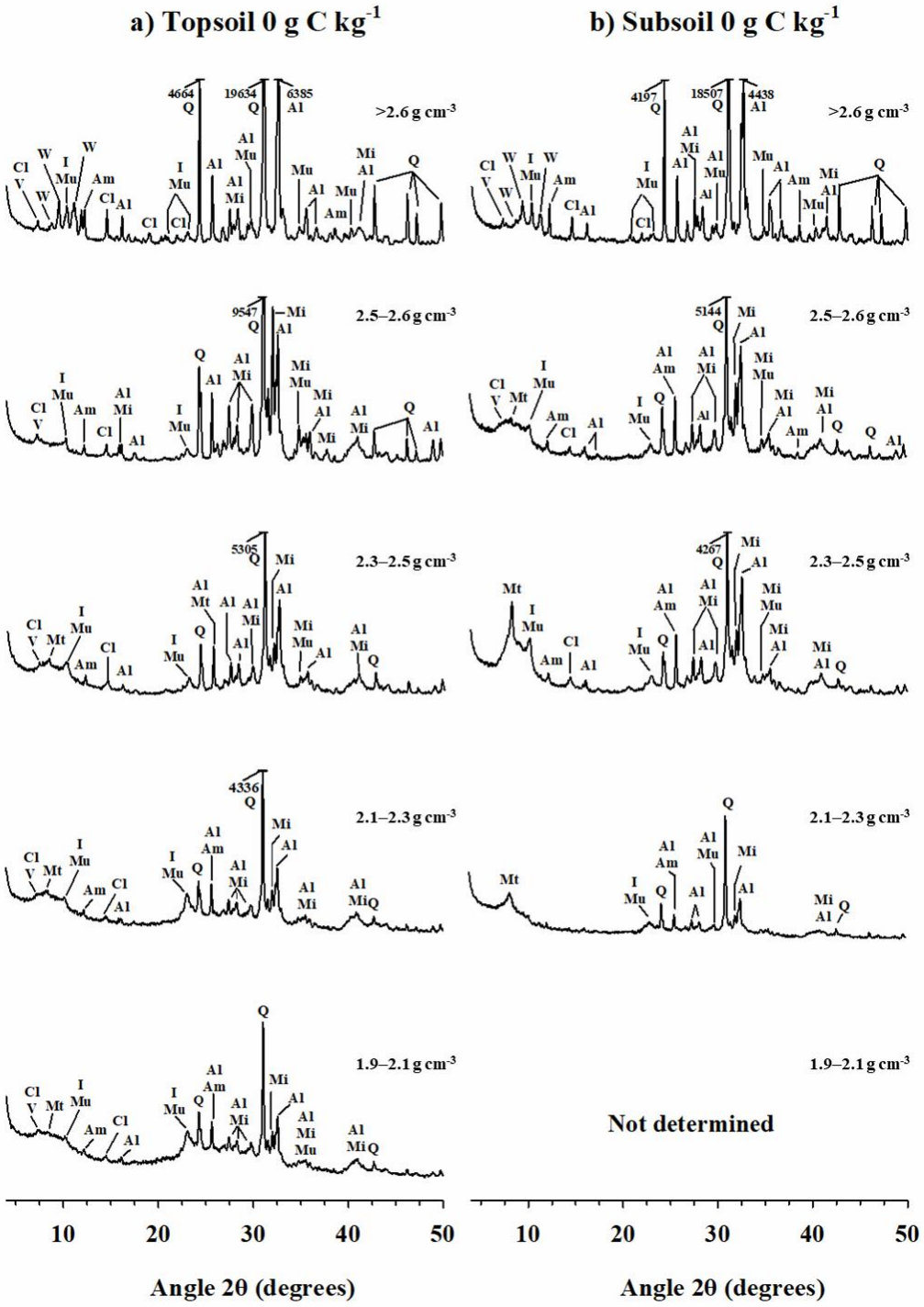

Figure 2. X-ray diffractograms (Co-Kα radiation) of soil density fractions in (**a**) topsoil and (**b**) subsoil that were incubated without residue. Mineralogical analysis of the subsoil 1.9–2.1 fraction is missing due to insufficient mass to analyze this fraction. All diffractograms are presented on the same vertical scale (intensity) and were truncated for legibility when the reading exceeded 4000 counts. The maximum number of counts is written next to the peak (Al, albite; Am, amphibole; Cl, chlorite; I, illite; Mi, microcline; Mu, muscovite; Mt, montmorillonite; Q, quartz; V, vermiculite; W, sodium polytungstate).

About one-third of residue-derived C (on average 1.95 g residue C kg^{-1} soil) and N (approximately 124.0 mg residue N kg^{-1} soil) were retained by the soil matrix in topsoil and subsoil. In the OLF fraction, there was more C from crop residue ($p = 0.04$) in topsoil than subsoil (Figure 4a), but similar amounts of N from crop residue in both soils (Figure 4b). Mineral-associated residue C (Residue C_{MAOM}, Equation (6)) was numerically greater ($p = 0.09$) in subsoil (0.64 g residue C kg^{-1} soil) than topsoil (0.52 g residue C kg^{-1} soil), and there was more ($p = 0.02$) mineral-associated residue N (Residue N_{MAOM}, Equation (6)) in subsoil (65.7 mg residue N kg^{-1} soil) than topsoil (48.2 mg residue N kg^{-1} soil). There was more ($p < 0.001$) residue C and N in the 2.3–2.5 fraction of topsoil than in subsoil, but the 2.5–2.6 and >2.6 fractions retained more ($p < 0.03$) residue C and N in subsoil than topsoil (Figure 4a,b). The proportions of residue-derived C and N retained by the soil matrix through organo-mineral interactions (Residue $C_{R\text{-}MAOM}$ and $N_{R\text{-}MAOM}$, Equation (7)) were greater ($p < 0.02$) in subsoil than topsoil (Figure 5). Residue C-to-residue N ratios were similar in all soil density fractions of these soils, except in the >2.6 fraction, which had a lower ($p = 0.007$) C/N ratio in the residues associated with subsoil than topsoil (Table 1).

Table 1. Recovery of residue C and residue N, and C/N and residue C-to-residue N ratios in density fractions in topsoil (0–20 cm) and subsoil (30–70 cm) incubated with 10 g C kg^{-1} soil of ^{13}C-^{15}N-labeled corn residues for 51 d.

Density Fractions ($g\ cm^{-3}$)	Distribution of Residue C (%)		Distribution of Residue N (%)		C/N		Residue C-to-Residue N Ratio	
	Topsoil	Subsoil	Topsoil	Subsoil	Topsoil	Subsoil	Topsoil	Subsoil
NOLF [1]	45.7 ^{Aa}[3]	40.5 ^{Aa}	16.7 ^{Aa}	18.8 ^{Aa}	21.6 ^{Aa}	19.2 ^{Ba}	35.7 ^{Aa}	30.5 ^{Aa}
OLF [2]	24.9 ^{Ab}	20.8 ^{Bb}	15.1 ^{Aa}	15.1 ^{Aa}	18.7 ^{Ab}	14.2 ^{Bb}	21.6 ^{Ab}	19.4 ^{Ab}
1.9–2.1	1.0 ^{Ad}	1.4 ^{Ad}	1.1 ^{Ac}	1.7 ^{Ab}	15.4 ^{Ac}	9.8 ^{Bc}	12.1 ^{Ad}	11.1 ^{Ac}
2.1–2.3	0.8 ^{Ae}	0.8 ^{Ae}	0.9 ^{Ac}	1.1 ^{Ad}	12.7 ^{Ad}	9.7 ^{Bc}	10.9 ^{Ae}	10.2 ^{Ac}
2.3–2.5	6.4 ^{Ac}	0.7 ^{Be}	8.1 ^{Ab}	1.0 ^{Bd}	9.5 ^{Af}	10.1 ^{Ac}	10.4 ^{Ae}	9.8 ^{Ac}
2.5–2.6	0.2 ^{Bf}	7.4 ^{Ac}	0.2 ^{Bd}	11.0 ^{Aa}	10.8 ^{Ae}	7.4 ^{Bd}	12.7 ^{Acde}	9.4 ^{Ac}
>2.6	0.2 ^{Bf}	0.4 ^{Af}	0.2 ^{Bd}	0.5 ^{Ae}	9.4 ^{Af}	7.9 ^{Ad}	15.4 ^{Ac}	10.7 ^{Bc}
All fractions	79.2 ^{A}	72.0 ^{A}	42.1 ^{A}	49.2 ^{A}	-	-	-	-

[1] NOLF = non-occluded light fraction ($\rho < 1.9$). [2] OLF = occluded light fraction ($\rho < 1.9$). [3] Means followed by different uppercase letters indicate a significant ($p < 0.05$) difference between topsoil and subsoil within density fractions, and means followed by different lowercase letters indicate a significant ($p < 0.05$) difference between density fractions within soil according to LSD test at $\alpha = 0.05$. C, carbon; N, nitrogen.

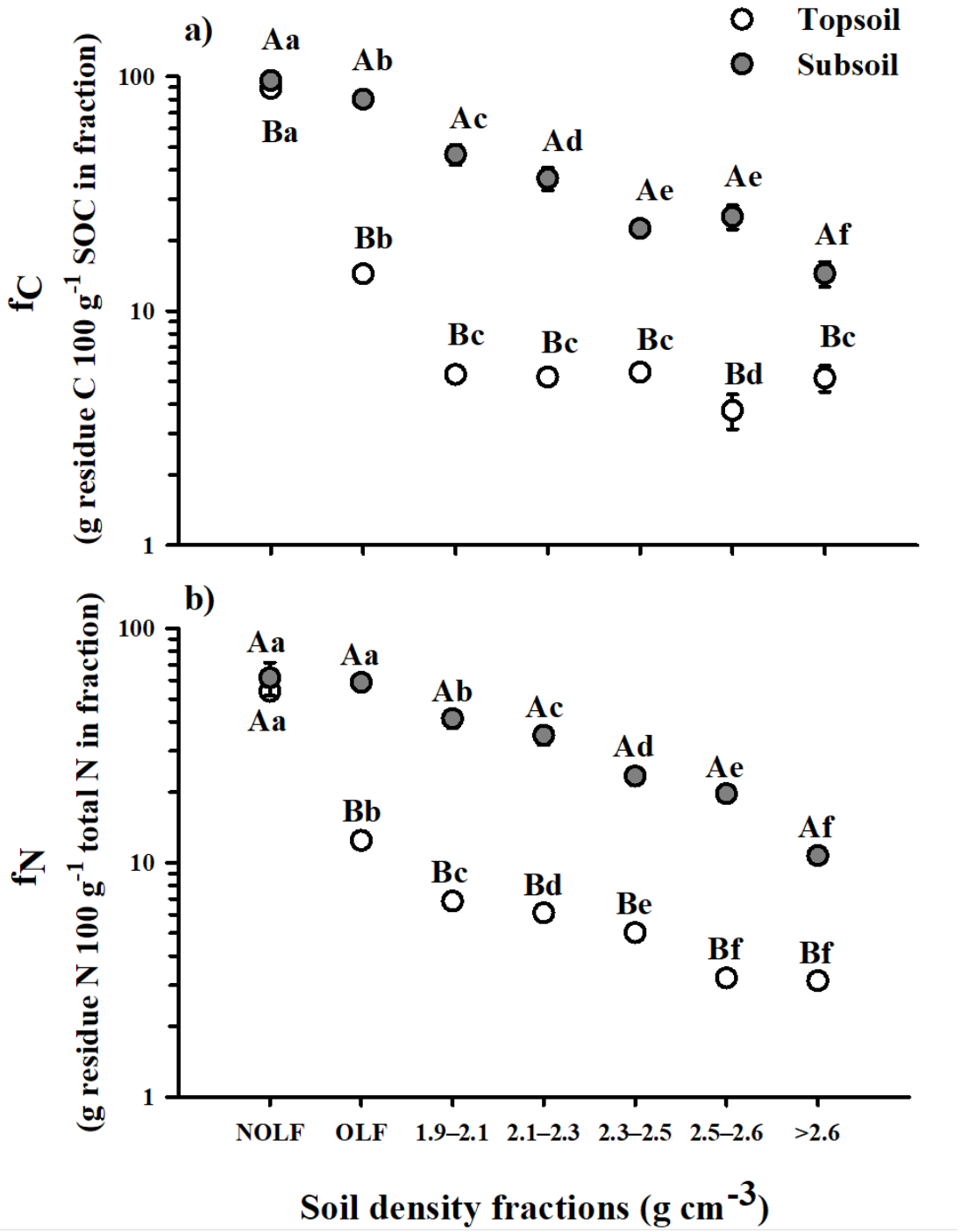

Figure 3. Fraction of (**a**) soil organic C (SOC) coming from residue C (f_C, Equation (4)) and (**b**) total soil N coming from residue N (f_N, Equation (4)) within density fractions in topsoil (0–20 cm) and subsoil (30–70 cm) after 51 d of incubation with 10 g C kg^{-1} of ^{13}C-^{15}N-labelled corn residues. Different uppercase letters indicate a significant difference between topsoil and subsoil within density fractions, and different lowercase letters indicate a significant difference between density fractions within soil according to Fisher's least significant difference (LSD) test.

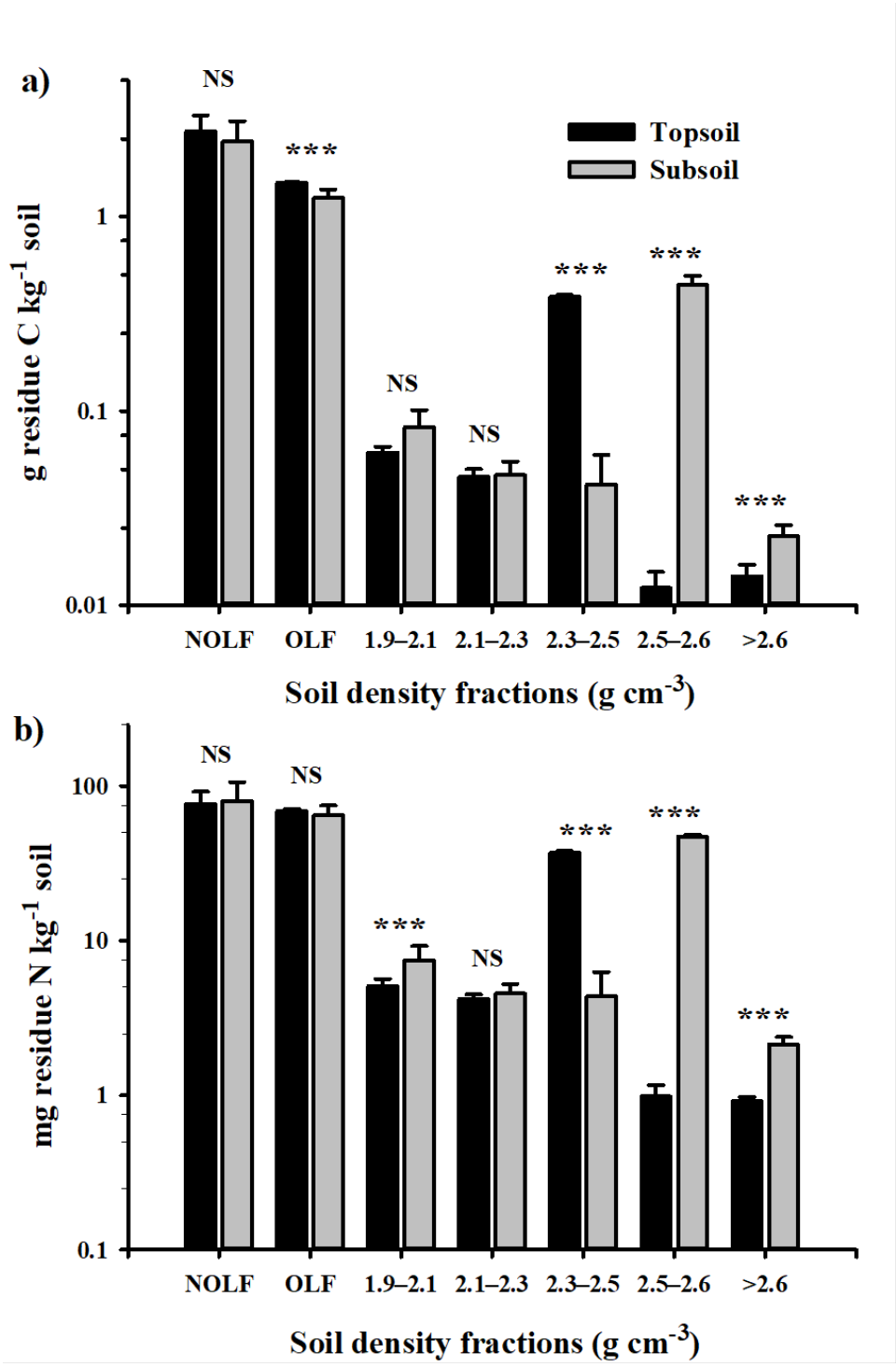

Figure 4. Concentrations of (**a**) residue C and (**b**) residue N in density fractions in topsoil (0–20 cm) and subsoil (30–70 cm) (Equation (5)) after 51 d of incubation with 10 g C kg^{-1} of ^{13}C-^{15}N-labelled corn residues. Error bars are standard deviation of the mean. NOFL, non-occluded light fraction ($\rho < 1.9$); OFL, occluded light fraction ($\rho < 1.9$). Within soil density fractions, NS indicates no significant difference and *, **, and *** indicate significant difference between topsoil and subsoil at $p < 0.05$, 0.01, and 0.001, respectively (LSD test). The *y*-axis is on a logarithmic scale.

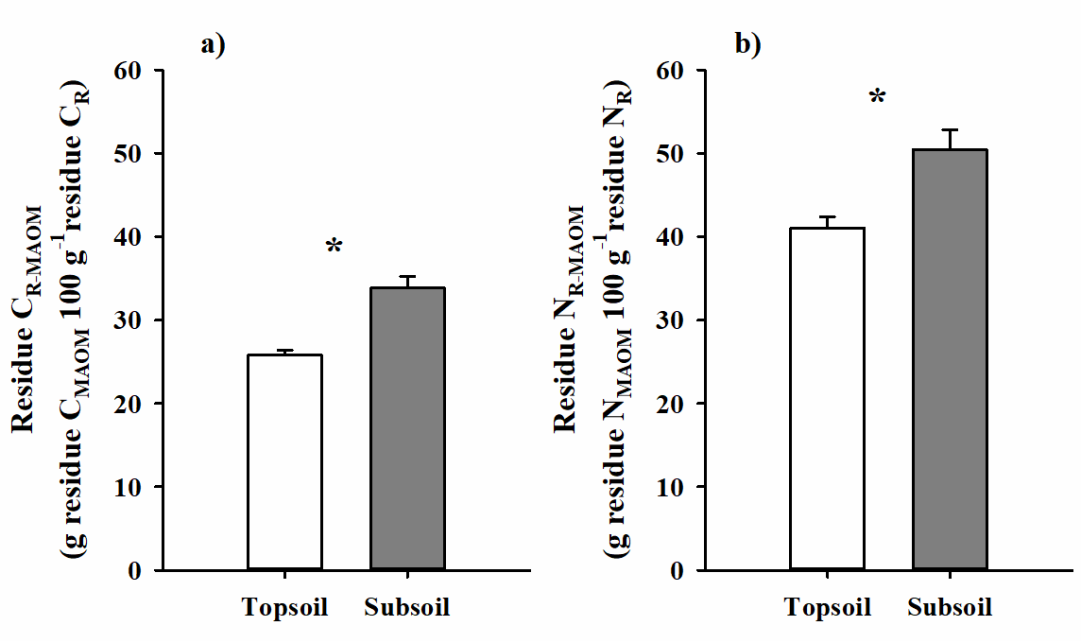

Figure 5. Proportions of (**a**) residue C and (**b**) residue N retained by the soil matrix in the form of mineral-associated organic matter (Residue $C_{R\text{-}MAOM}$ and Residue $N_{R\text{-}MAOM}$, Equation (7)) in topsoil (0–20 cm) and subsoil (30–70 cm) from a heavy clay incubated for 51 d with 10 g C kg^{-1} of ^{13}C-^{15}N-labelled corn residues. * indicates significant difference at p <0.05 between topsoil and subsoil.

4. Discussion

4.1. Methodological Considerations

We chose a density solution of 1.9 to separate uncomplexed NOLF and OLF from mineral-associated SOM in organo-mineral complexes. This threshold is consistent with other reports of SOM density fractionation [30,31]. However, we detected trace amounts of minerals in the XRD scans of NOLF and OLF (data not shown), possibly because minerals are also adsorbed on SOM in NOLF and OLF [32]. Therefore, the NOLF and OLF in this study were not composed exclusively of physically uncomplexed organic matter in the sense used by Gregorich et al. [30]. The recovery of ~88% of total soil mass in density fractions is similar to Basile-Doelsch et al. [16] and Bonnard et al. [33], but lower than Swanston et al. [34] and Plante et al. [35], who recovered ~100% soil mass.

The missing soil mass could be in particles <0.2 μm, which can represent up to 30% of the clays in the heavy clay soils of Eastern Canada [10,36]. Suspended clays remaining in the density solution that were not recovered by our centrifugation procedure could contain an appreciable amount of C and N, since we recovered about 76% and 46% of residue-derived C and N, respectively. It is not unusual to achieve less than 100% SOM recovery during density separation [17,33,35]. In this study, the losses of residue C and N may be due to (1) SOM solubilization by water and polytungstate solutions (despite their close-to-neutral pH), (2) SOM association with clay particles <0.2 μm, which were not recovered, and (3) SOM dispersion by sonication during rinsing steps (as seen by the dark color of rinsing water, particularly in the OLF, 2.3–2.5, and 2.5–2.6 fractions). Despite these methodological constraints, the quantities of soil and residue-derived C and N recovered during sequential density separation were sufficient to evaluate the quantity of occluded and mineral-associated SOM derived from the corn residue.

4.2. Residue-Derived C and N Retention in Occluded SOM

The OLF was much richer in residue-derived C and N in the subsoil than in the topsoil (Figure 3). However, its mass in proportion of the whole soil (i.e., g OLF kg^{-1} soil, data not shown) was eight times lower in subsoil than in topsoil. Consequently, the concentration of OLF-associated residue C on a whole soil basis (i.e., g residue C in OLF kg^{-1} soil, Figure 4a) was slightly greater in topsoil than subsoil, but both soils had similar amounts of residue N in this fraction (Figure 4b). The difference between the two elements could be because N is recycled in the soil during microbial processes, leading to N occlusion in soil aggregates, whereas C is partly lost as CO_2. The subsoil was thus highly responsive to residue addition, achieving greater occlusion of C and N from crop residue than topsoil in the 51 d incubation. This is consistent with our previous observation of greater retention of residue-derived C and N in particulate organic matter within macroaggregates >1000 μm, as well as greater macroaggregation per unit C added, in subsoil than topsoil [19].

4.3. Residue-Derived C and N Retention in Mineral-Associated SOM

As hypothesized, the retention of residue-derived C and N in mineral-associated SOM was greater in subsoil than topsoil. The hypothesis was confirmed when we evaluated the absolute amount of residue (Residue C_{MAOM} and N_{MAOM}, Equation (6), Section 3.3) or the proportion of residue retained by the soil matrix (Residue $C_{R\text{-}MAOM}$ and $N_{R\text{-}MAOM}$, Equation (7), Figure 5a,b). This indicates that mineral surfaces in subsoil can retain more C and N than minerals in topsoil [20,22,37,38]. In the topsoil, most of the mineral-associated residue C and N was found in the 2.3–2.5 fraction, whereas in the subsoil, residue C and N were mostly retained in the 2.5–2.6 fraction. However, the topsoil 2.3–2.5 fraction and the subsoil 2.5–2.6 fraction showed similar diffractograms. Diffusion bands at low angle could be caused by poorly crystalline amorphous material, interstratification, or overlapping of peaks of minerals that are increasingly more expansive [16,32,35,39]. The greater diffusion bands at low angle in topsoil fractions <2.5 suggest that this soil could contain more amorphous, interstratified, or expansible minerals than the subsoil. Perhaps the more intense rhizospheric activity increased mineral weathering in the topsoil and caused the enrichment compared to the subsoil [40]. Minerals stabilizing SOM in the topsoil 2.3–2.5 and the subsoil 2.5–2.6 fractions are most likely illite, chlorite, vermiculite, montmorillonite, interstratified minerals, and amorphous material (see Figure 2). The potential of these minerals to stabilize residue-derived C and N is influenced by external and internal (for swelling minerals like vermiculite and montmorillonite) specific surface area (SSA, in $m^2\ g^{-1}$) and cation exchange capacity (CEC, in $cmol_+\ kg^{-1}$) [41,42]. The SSA and CEC are, respectively, 70 to 175 $m^2\ g^{-1}$ and 10 to 40 $cmol_+\ kg^{-1}$ for illite + chlorite, 200 $m^2\ g^{-1}$ and 150 to 200 $cmol_+\ kg^{-1}$ for amorphous material, 70 to 120 $m^2\ g^{-1}$ (external) + 600 to 700 $m^2\ g^{-1}$ (internal) and 100 to 200 $cmol_+\ kg^{-1}$ for vermiculite, and 80 to 150 $m^2\ g^{-1}$ (external) + 550 to 650 $m^2\ g^{-1}$ (internal) and 80 to 150 $cmol_+\ kg^{-1}$ for montmorillonite [10,42]. Interstratified minerals represent intermediate transformation products, most likely in the form of illite–montmorillonnite and/or chlorite–vermiculite [43,44], and likely have intermediate capacity to stabilize residue-derived C and N. De Kimpe et al. [10] found that the Kamouraska soil contains ~44% illite + chlorite, ~15% montmorillonnite, ~7% vermiculite, and ~5% amorphous material, and Kodama et al. [40] found that interstratified minerals represented ~4% of the Dalhousie soil, a similiar gleysol formed on marine clay in Eastern Canada. We therefore postulate that mineral-associated residue C and N in topsoil 2.3–2.5 and subsoil 2.5–2.6 fractions were retained by forming organo-mineral complexes with illite + chlorite > montmorillonite > vermiculite > interstatified minerals = amorphous material. In the SOM-poor subsoil, mineral surfaces were less associated with organic compounds and organo-mineral complexes remained in a heavier density fraction (i.e., 2.5–2.6). In the SOM-rich topsoil, higher coverage of mineral surfaces decreased the density of organo-mineral complexes, which were found in a lower density fraction (2.3–2.5). This is consistent with the postulate that mineral surfaces are less associated with organic compounds in subsoil than topsoil.

Residue-derived C and N were retained by the same minerals in topsoil and subsoil, particularly in association with illite + chlorite and montmorillonite. However, residue N was retained preferentially through organo-mineral interactions, particularly in the subsoil. The evidence for this is (1) the greater proportion of whole-soil residue N than whole-soil residue C in organo-mineral complexes (Table 1) and (2) the higher values for Residue $N_{R\text{-}MAOM}$ than Residue $C_{R\text{-}MAOM}$ (Figure 5a,b, Equation (7)). This may suggest preferential adsorption of N-containing biomolecules [8,14,45] on illite and montmorillonite. Montmorillonitic soils retain peptides and become enriched with amine-N [46,47]. Microbial residues such as secretions and necromass are a component of mineral-associated SOM [31,48] although Vogel et al. [49] reported that illite retained more microbial-derived C and N than montmorillonite. Finally, residue N could be mineralized to $^{15}N\text{-}NH_4^+$, which is then adsorbed onto mineral surfaces or retained into siloxane cavities from montmorillonite surfaces [19,32,50].

The subsoil >2.6 fraction preferentially retained the residue N, based on its lower residue C-to-residue N ratio than other fractions. Hatton et al. [51] found more microbial residues in the mineral grain fraction correponding to a 2.4–2.65 density fraction, and postulated that the mineral grains were a preferential habitat for soil microorganisms. The >2.6 fraction in the subsoil contained illite, chlorite, and traces of vermiculite, which could support soil microbial biomass or bind microbial byproducts. This fraction also contained amphibole, a Fe-bearing mineral. Since Fe coating on primary minerals is expected to increase their sorption potential [32], perhaps amphibole also contributed, at least partly, to retain residue-derived C and N in the subsoil >2.6 fraction.

5. Conclusions

Organo-mineral interactions were more important for the retention of residue-derived C and N in the subsoil than the topsoil, but an appreciable amount of residue-derived C and N was also retained through occlusion in the subsoil. Minerals such as illite + chlorite, montmorillonite, vermiculite, and amorphous material are important for the retention of residue C and N in topsoil and subsoil, but they are found in different density fractions, mainly in the 2.3–2.5 fraction of topsoil and the 2.5–2.6 fraction in subsoil. Finally, mineral-associated SOM was enriched in residue N in subsoil, likely because of greater reactive mineral surface area than in the topsoil. This confirms that low SOM concentration promotes the short-term stabilization of newly added material. Further research should investigate the microbial processing and the molecular nature of mineral-associated residue C and N in topsoil and subsoil. Since this work evaluated the short-term stabilization of residue-derived C and N, a next step could be to evaluate the long-term persistance of recently added C and N retained through organo-mineral intertactions in topsoil and subsoil. In conclusion, our results suggest that in soils with high clay content and reactive minerals, and low autochthonous SOM concentration, residue-derived C and N are rapidly stabilized into mineral-associated organic matter.

Author Contributions: Conceptualization, V.P. and D.A.A.; Formal analysis, V.P.; Funding acquisition, V.P., J.K.W., and D.A.A.; Investigation, V.P. and I.B.-D.; Methodology, V.P., I.B.-D., D.B., and D.A.A.; Project administration, I.B.-D., J.B., J.K.W., and D.A.A.; Resources, I.B.-D., J.B., J.K.W. and D.A.A.; Supervision, I.B.-D., J.B., J.K.W., and D.A.A.; Visualization, V.P.; Writing—original draft, V.P.; Writing—review and editing, V.P., I.B.-D., J.B., D. B., J.K.W., and D.A.A. All authors have read and agreed to the published version of the manuscript.

Funding: This research was funded by the Fonds de recherche du Québec—Nature et technologie (FRQNT), the Max Bell Foundation at McGill University, and the National Science and Engineering Research Council (NSERC) of Canada through postgraduate scholarships awarded to V.P., The Green Crop Network, funded by NSERC (grant number NETGP298866-03), and the Centre SEVE, funded by the FRQNT Strategic Networks program.

Acknowledgments: The authors would like to thank Agriculture and Agri-Food Canada staff for the technical assistance provided, in particular Normand Bertrand, Gabriel Lévesque, Johanne Tremblay, and Nicole Bissonnette. The authors are also thankful to two anonymous reviewers for their helpful comments and the time they allotted to revising a previous version of this manuscript.

Conflicts of Interest: The authors declare no conflict of interest.

Appendix A

The density of organo-mineral complexes (ρ_{cpx} in g cm^{-3}) was calculated as follows:

$$\rho_{cpx} = M_{cpx} \div [V_{mx} + V_{om}], \quad \text{(A1)}$$

where M_{cpx} is the mass of the organo-mineral complex (set at 1 g for calculation purposes), and V_{mx} and V_{om} are the volumes (in cm^3) of the mineral and organic matter in 1 g of organo-mineral complex, respectively. Density (ρ) values are reported without stating g cm^{-3}. The volume of mineral (V_{mx}, in cm^3) in 1 g of organo-mineral complex was as follows:

$$V_{mx} = [1 - (1.7 * SOC_{cpx})] \div \rho_{mx}, \quad \text{(A2)}$$

where 1.7 is a factor proposed by Baldock and Nelson [52] to convert SOC concentration into SOM content (g SOM g^{-1} SOC), SOC_{cpx} is organo-mineral complex theoretical SOC concentration (mg SOC g^{-1} organo-mineral complex), and ρ_{mx} is mineral density. Minerals were separated in two groups: the first included quartz, microcline, albite, and amphibole (Table A1), which have low specific surface area (SSA), and the second comprised chlorite, vermiculite, and illite/muscovite, which have moderate to high SSA (Table A2) [10]. We used theoretical SOC_{cpx} values of 0, 25, and 50 mg SOC g^{-1} organo-mineral complex for minerals of the first group and 50, 100, and 200 mg SOC g^{-1} organo-mineral complex for minerals of the second group, to calculate V_{mx}. We also used minimum, average, and maximum values for ρ_{mx} taken from the literature (see Tables A1 and A2). The volume of organic matter (V_{om}, in cm^3) in 1 g of organo-mineral complex was calculated as follows:

$$V_{om} = [1.7 * (SOC_{cpx}/1000)] \div \rho_{om}, \quad \text{(A3)}$$

where ρ_{om} is the density of soil organic matter (i.e., 1.6 according to Chenu and Plante [53]). Our procedure yielded nine estimated values of ρ_{cpx} for each mineral, resulting in a mean ρ value (and standard deviation) for each mineral (Tables A1 and A2). We chose 1.9 as the initial density threshold after Gregorich et al. [30] and Basile-Doelsch et al. [16]. From the ρ_{cpx} estimates, we set five density thresholds for the sequential fractionation, that is, ρ = 1.9, 2.1, 2.3, 2.5, and 2.6 (Figure A1).

Table A1. Estimation of organo-mineral complex density for minerals having a low specific surface area.

Quartz										
ρ_{mx} (g cm^{-3}) †	**2.62**			**2.65**			**2.66**			**Mean (SD)**
SOC_{cpx} (mg SOC g^{-1} cpx) ¶	**0**	**25**	**50**	**0**	**25**	**50**	**0**	**25**	**50**	
V_{om} (cm^3) ‡	0.000	0.027	0.053	0.000	0.027	0.053	0.000	0.027	0.053	-
V_{mx} (cm^3) ∫	0.382	0.365	0.349	0.378	0.362	0.346	0.376	0.360	0.344	-
ρ_{cpx} (g cm^{-3}) §	2.620	2.551	2.485	2.647	2.576	2.508	2.660	2.584	2.518	2.572 (0.062)
Microcline										
ρ_{mx} (g cm^{-3})	**2.44**			**2.55**			**2.60**			**Mean (SD)**
SOC_{cpx} (mg SOC g^{-1} cpx)	**0**	**25**	**50**	**0**	**25**	**50**	**0**	**25**	**50**	
V_{om} (cm^3)	0.000	0.027	0.053	0.000	0.027	0.053	0.000	0.027	0.053	-
V_{mx} (cm^3)	0.410	0.392	0.375	0.393	0.376	0.359	0.385	0.368	0.352	-
ρ_{cpx} (g cm^{-3})	2.440	2.387	2.336	2.547	2.484	2.425	2.600	2.533	2.469	2.469 (0.083)
Albite										
ρ_{mx} (g cm^{-3})	**2.59**			**2.62**			**2.64**			**Mean (SD)**
SOC_{cpx} (mg SOC g^{-1} cpx)	**0**	**25**	**50**	**0**	**25**	**50**	**0**	**25**	**50**	
V_{om} (cm^3)	0.000	0.027	0.053	0.000	0.027	0.053	0.000	0.027	0.053	-
V_{mx} (cm^3)	0.386	0.370	0.353	0.382	0.366	0.350	0.379	0.363	0.347	-
ρ_{cpx} (g cm^{-3})	2.590	2.524	2.461	2.618	2.549	2.483	2.640	2.569	2.502	2.548 (0.061)
Amphibole										
ϱ_{mx} (g cm^{-3})	**2.59**			**2.62**			**2.64**			**Mean (SD)**
SOC_{cpx} (mg SOC g^{-1} cpx)	**0**	**25**	**50**	**0**	**25**	**50**	**0**	**25**	**50**	
V_{om} (cm^3)	0.000	0.027	0.053	0.000	0.027	0.053	0.000	0.027	0.053	-
V_{mx} (cm^3)	0.334	0.320	0.306	0.313	0.300	0.286	0.303	0.290	0.277	-
ρ_{cpx} (g cm^{-3})	2.990	2.884	2.784	3.195	3.065	2.945	3.300	3.157	3.027	3.039 (0.161)

† Minimum, average, and maximum values for mineral density (ρ_{mx}) taken from Battey [54], Barthelmy [55], Deer et al. [56], Fischenner [57], Jouenne [58], Mincryst [59], Mindat [60], and [27]. ¶ Theoretical soil

organic carbon concentration of organo-mineral complex (SOC_{cpx}). ‡ Volume of organic matter (V_{om}) in 1 g organo-mineral complex calculated after Equation (A3). ∫ Volume of mineral (V_{mx}) in 1 g organo-mineral complex calculated after Equation (A2). § Organo-mineral complex density (ρ_{cpx}) calculated after Equation (A1). The mean values (and standard deviation) presented in the last column were used to determine density thresholds for the separation protocol.

Table A2. Estimation of organo-mineral complex density for minerals having a high specific surface area.

Chlorite										
ρ_{mx} (g cm^{-3}) †	**2.65**			**2.83**			**2.95**			**Mean (SD)**
SOC_{cpx} (mg SOC g^{-1} cpx) ¶	**50**	**100**	**200**	**50**	**100**	**200**	**50**	**100**	**200**	
V_{om} (cm^3) ‡	0.053	0.106	0.213	0.053	0.106	0.213	0.053	0.106	0.213	-
V_{mx} (cm^3) ∫	0.345	0.313	0.249	0.323	0.293	0.233	0.310	0.281	0.224	-
ρ_{cpx} (g cm^{-3}) §	2.510	2.384	2.167	2.659	2.505	2.245	2.753	2.580	2.292	2.455 (0.197)
Vermiculite										
ρ_{mx} (g cm^{-3})	**2.30**			**2.37**			**2.50**			**Mean (SD)**
SOC_{cpx} (mg SOC g^{-1} cpx)	**50**	**100**	**200**	**50**	**100**	**200**	**50**	**100**	**200**	
V_{om} (cm^3)	0.053	0.106	0.213	0.053	0.106	0.213	0.053	0.106	0.213	-
V_{mx} (cm^3)	0.398	0.361	0.287	0.386	0.350	0.278	0.366	0.332	0.264	-
ρ_{cpx} (g cm^{-3})	2.218	2.141	2.002	2.277	2.191	2.037	2.386	2.282	2.099	2.181 (0.184)
Illite/Muscovite										
ρ_{mx} (g cm^{-3})	**2.70**			**2.83**			**2.90**			**Mean (SD)**
SOC_{cpx} (mg SOC g^{-1} cpx)	**50**	**100**	**200**	**50**	**100**	**200**	**50**	**100**	**200**	
V_{om} (cm^3)	0.053	0.106	0.213	0.053	0.106	0.213	0.053	0.106	0.213	-
V_{mx} (cm^3)	0.339	0.307	0.244	0.323	0.293	0.233	0.316	0.286	0.228	-
ρ_{cpx} (g cm^{-3})	2.551	2.417	2.188	2.713	2.548	2.272	2.656	2.503	2.244	2.455 (0.186)

† Minimum, average, and maximum values for mineral density (ρ_{mx}) taken from Battey [54], Barthelmy [55], Deer et al. [56], Fischenner [57], Jouenne [58], Mincryst [59], Mindat [60], and [27]. ¶ Theoretical soil organic carbon concentration of organo-mineral complex (SOC_{cpx}). ‡ Volume of organic matter (V_{om}) in 1 g organo-mineral complex calculated after Equation (A3). ∫ Volume of mineral (V_{mx}) in 1 g organo-mineral complex calculated after Equation (A2). § Organo-mineral complex density (ρ_{cpx}) calculated after Equation (A1). The mean values (and standard deviation) presented in the last column were used to determine density thresholds for the separation protocol.

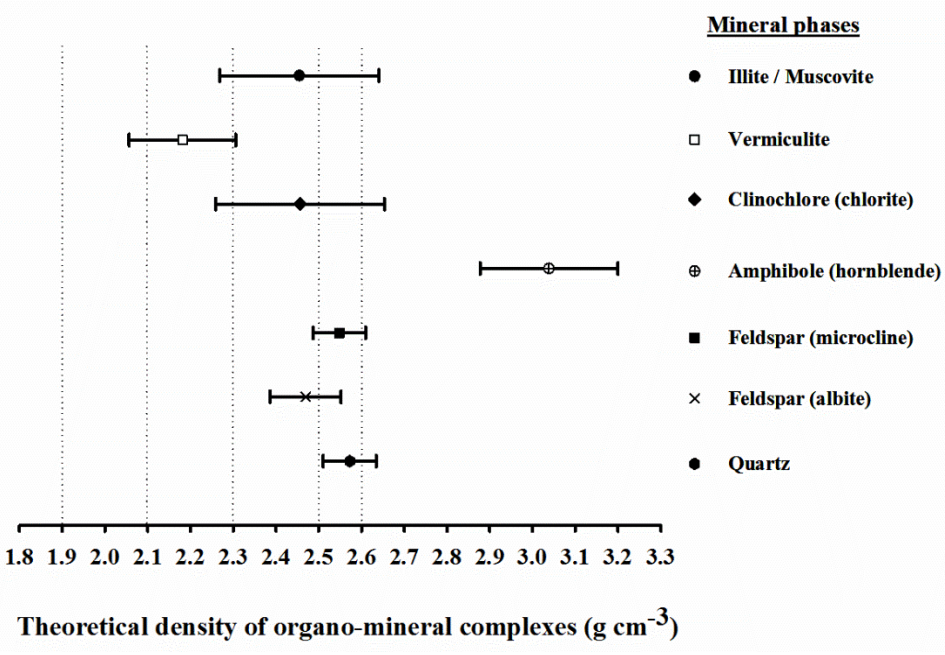

Figure A1. Theoretical densities of organo-mineral complexes associated with soil minerals. Horizontal bars are standard deviations from the means calculated in Tables A1 and A2 (see above). Dotted lines are thresholds for the sequential density separation.

References

1. Derrien, D.; Dignac, M.-F.; Basile-Doelsch, I.; Barot, S.; Cécillon, L.; Chenu, C.; Chevallier, T.; Freschet, G.T.; Garnier, P.; Guenet, B.; et al. Stocker du C dans les sols : Quels mécanismes, quelles pratiques agricoles, quels indicateurs ? *Étude Gest. des sols* **2016**, *23*, 193–224.
2. Paustian, K.; Lehmann, J.; Ogle, S.; Reay, D.; Robertson, G.P.; Smith, P. Climate-smart soils. *Nature* **2016**, *532*, 49–57.
3. Chen, S.; Martin, M.P.; Saby, N.P.A.; Walter, C.; Angers, D.A.; Arrouays, D. Fine resolution map of top- and subsoil carbon sequestration potential in France. *Sci. Total Environ.* **2018**, *630*, 389–400.
4. Golchin, A.; Oades, J.M.; Skjemstad, J.O.; Clarke, P. Soil structure and carbon cycling. *Aust. J. Soil Res.* **1994**, *32*, 1043–1068.
5. Baldock, J..; Skjemstad, J.. Role of the soil matrix and minerals in protecting natural organic materials against biological attack. *Org. Geochem.* **2000**, *31*, 697–710.
6. von Lützow, M.; Kögel-Knabner, I.; Ekschmitt, K.; Matzner, E.; Guggenberger, G.; Marschner, B.; Flessa, H. Stabilization of organic matter in temperate soils: mechanisms and their relevance under different soil conditions - a review. *Eur. J. Soil Sci.* **2006**, *57*, 426–445.
7. von Lützow, M.; Kögel-Knabner, I.; Ekschmitt, K.; Flessa, H.; Guggenberger, G.; Matzner, E.; Marschner, B. SOM fractionation methods: Relevance to functional pools and to stabilization mechanisms. *Soil Biol. Biochem.* **2007**, *39*, 2183–2207.
8. Kleber, M.; Sollins, P.; Sutton, R. A conceptual model of organo-mineral interactions in soils : self-assembly of organic molecular fragments into zonal structures on mineral surfaces. *Biogeochemistry* **2007**, *85*, 9–24.
9. Moni, C.; Derrien, D.; Hatton, P.-J.; Zeller, B.; Kleber, M. Density fractions versus size separates: does physical fractionation isolate functional soil compartments? *Biogeosciences* **2012**, *9*, 5181–5197.
10. De Kimpe, C.; Laverdière, M.; Martel, Y. Surface area and exchange capacity of clay in relation to the mineralogical composition of gleysolic soils. *Can. J. Soil Sci.* **1979**, *59*, 341–347.
11. Monreal, C.M.; Schulten, H.-R.; Kodama, H. Age, turnover and molecular diversity of soil organic matter in aggregates of a Gleysol. *Can. J. Soil Sci.* **1997**, *77*, 379–388.
12. Hassink, J. The capacity of soils to preserve organic C and N by their association with clay and silt particles. *Plant Soil* **1997**, *191*, 77–87.
13. Carter, M.R.; Angers, D.A.; Gregorich, E.G.; Bolinder, M.A. Characterizing organic matter retention for surface soils in eastern Canada using density and particle size fractions. *Can. J. Soil Sci.* **2003**, *83*, 11–23.
14. Sollins, P.; Swanston, C.; Kleber, M.; Filley, T.; Kramer, M.; Crow, S.; Caldwell, B. a.; Lajtha, K.; Bowden, R. Organic C and N stabilization in a forest soil: Evidence from sequential density fractionation. *Soil Biol. Biochem.* **2006**, *38*, 3313–3324.
15. Gunina, A.; Kuzyakov, Y. Pathways of litter C by formation of aggregates and SOM density fractions: Implications from 13C natural abundance. *Soil Biol. Biochem.* **2014**, *71*, 95–104.
16. Basile-Doelsch, I.; Amundson, R.; Stone, W.E.E.; Borschneck, D. Mineral control of carbon pools in a volcanic soil horizon. *Geoderma* **2007**, *137*, 477–489.
17. Basile-Doelsch, I.; Brun, T.; Borschneck, D.; Masion, A.; Marol, C.; Balesdent, J. Effect of landuse on organic matter stabilized in organomineral complexes : A study combining density fractionation , mineralogy and δ 13 C. *Geoderma* **2009**, *151*, 77–86.

18. Gregorich, E.G.; Carter, M.R.; Angers, D.A.; Drury, C.F. Using a sequential density and particle-size fractionation to evaluate carbon and nitrogen storage in the profile of tilled and no-till soils in eastern Canada. *Can. J. Soil Sci.* **2009**, *89*, 255–267.
19. Poirier, V.; Angers, D.A.; Whalen, J.K. Formation of millimetric-scale aggregates and associated retention of 13C-15N-labelled residues are greater in subsoil than topsoil. *Soil Biol. Biochem.* **2014**, *75*, 45–53.
20. Stewart, C.; Paustian, K.; Conant, R.; Plante, A.; Six, J. Soil carbon saturation: Evaluation and corroboration by long-term incubations. *Soil Biol. Biochem.* **2008**, *40*, 1741–1750.
21. Poirier, V.; Angers, D.A.; Rochette, P.; Whalen, J.K. Initial soil organic carbon concentration influences the short-term retention of crop-residue carbon in the fine fraction of a heavy clay soil. *Biol. Fertil. Soils* **2013**, *49*, 527–535.
22. Kaiser, K.; Guggenberger, G. Mineral surfaces and soil organic matter. *Eur. J. Soil Sci.* **2003**, *54*, 219–236.
23. Lorenz, K.; Lal, R. The depth distribution of soil organic carbon in relation to land use and management and the potential of carbon sequestration in subsoil horizons. *Adv. Agron.* **2005**, *88*, 35–66.
24. IUSSS Working Group WRB *World Reference Base for Soil Resources, Second edition. World Soil Resources Report No. 103*; FAO: Rome, 2006; ISBN 9251055114.
25. Soil Classification Working Group *The Canadian System of Soil Classification. Third Edition*; Agriculture and Agri-Food Canada Publication No. 1646, National Research Council of Canada: Ottawa, 1998;
26. Pangea UK *LST Fastfloat - technical brochure*; Chippenham, Wilts, United Kingdom, 2006;
27. PANanlytical BV X'Pert High Score Software version 3.0, PANalytical B.V.: Alamo, Netherlands 2009.
28. SAS Institute Inc. SAS/STAT for Windos version 9.2, SAS: Cary, NC, USA, 2002.
29. Systat Software Inc. SigmaPlot for Windows version 13.0, Systat Software Inc.: San Jose, CA, USA, 2014.
30. Gregorich, E.G.; Beare, M.H.; Mckim, U.F.; Skjemstad, J.O. Chemical and biological characteristics of physically uncomplexed organic matter. *Soil Sci. Soc. Am. J.* **2006**, *70*, 975–985.
31. Ludwig, M.; Achtenhagen, J.; Miltner, A.; Eckhardt, K.; Leinweber, P.; Emmerling, C.; Thiele-Bruhn, S. Microbial contribution to SOM quantity and quality in density fractions of temperate arable soils. *Soil Biol. Biochem.* **2015**, *81*, 311–322.
32. Sollins, P.; Kramer, M.G.; Swanston, C.; Lajtha, K.; Filley, T.; Aufdenkampe, A.K.; Wagai, R.; Bowden, R.D. Sequential density fractionation across soils of contrasting mineralogy: evidence for both microbial- and mineral-controlled soil organic matter stabilization. *Biogeochemistry* **2009**, *96*, 209–231.
33. Bonnard, P.; Basile-Doelsch, I.; Balesdent, J.; Masion, A.; Borschneck, D.; Arrouays, D. Organic matter content and features related to associated mineral fractions in an acid, loamy soil. *Eur. J. Soil Sci.* **2012**, *63*, 625–636.
34. Swanston, C.; Torn, M.; Hanson, P.; Southon, J.; Garten, C.; Hanlon, E.; Ganio, L. Initial characterization of processes of soil carbon stabilization using forest stand-level radiocarbon enrichment. *Geoderma* **2005**, *128*, 52–62.
35. Plante, A.; Virto, I.; Malhi, S. Pedogenic, mineralogical and land-use controls on organic carbon stabilization in two contrasting soils. *Can. J. Soil Sci.* **2010**, *90*, 15–26.
36. Martel, Y.; De Kimpe, C.; Laverdière, M. Cation-exchange capacity of clay-rich soils in relation to organic matter, mineral composition and surface area. *Soil Sci. Soc. Am. J.* **1978**, *42*, 764–767.
37. Rasse, D.; Rumpel, C.; Dignac, M.-F. Is soil carbon mostly root carbon? Mechanisms for a specific stabilisation. *Plant Soil* **2005**, *269*, 341–356.

38. Castellano, M.J.; Kaye, J.P.; Lin, H.; Schmidt, J.P. Linking carbon saturation concepts to nitrogen saturation and retention. *Ecosystems* **2012**, *15*, 175–187.
39. Kodama, H. Clay minerals in Canadian soils: Their origin, distribution and alteration. *Can. J. Soil Sci.* **1979**, *59*, 37–58.
40. Kodama, H.; Nelson, S.; Yang, A.; Kohyama, N. Mineralogy of rhizospheric and non-rhizospheric soils in corn fields. *Clays Clay Miner.* **1994**, *42*, 755–763.
41. Sarkar, B.; Singh, M.; Mandal, S.; Churchman, G.J.; Bolan, N.S. Clay minerals-organic matter interactions in relation to carbon stabilization in soils. In *The Future of Soil Carbon: Its Conservation and Formation*; Garcia, C., Nannipieri, P., Hernandez, T., Eds.; Elsevier Inc.: Amsterdam, Netherlands, 2018; pp. 71–86 ISBN 9780128116876.
42. Brady, N.; Weil, R. *Elements of the nature and properties of soils. Second edition*; Pearson Education: Upper Saddle River, USA, 2004;
43. Wilson, M.J. The origin and formation of clay minerals in soils: past, present and future perspectives. *Clay Miner.* **1999**, *34*, 7–25.
44. Churchman, G.J. Is the geological concept of clay minerals appropriate for soil science? A literature-based and philosophical analysis. *Phys. Chem. Earth* **2010**, *35*, 927–940.
45. Feng, X.; Simpson, A.; Simpson, M. Chemical and mineralogical controls on humic acid sorption to clay mineral surfaces. *Org. Geochem.* **2005**, *36*, 1553–1566.
46. Block, K.A.; Trusiak, A.; Katz, A.; Alimova, A.; Wei, H.; Gottlieb, P.; Steiner, J.C. Applied Clay Science Exfoliation and intercalation of montmorillonite by small peptides. *Appl. Clay Sci.* **2015**, *107*, 173–181.
47. Jindaluang, W.; Kheoruenromne, I.; Suddhiprakarn, A.; Pal Singh, B.; Singh, B. Influence of soil texture and mineralogy on organic matter content and composition in physically separated fractions soils of Thailand. *Geoderma* **2013**, *195–196*, 207–219.
48. Singh, B.P.; Hatton, B.J.; Singh, B.; Cowie, A.L.; Kathuria, A. Influence of Biochars on Nitrous Oxide Emission and Nitrogen Leaching from Two Contrasting Soils. *J. Environ. Qual.* **2010**, *39*, 1224.
49. Vogel, C.; Heister, K.; Buegger, F.; Tanuwidjaja, I.; Haug, S.; Schloter, M.; Kögel-knabner, I. Clay mineral composition modifies decomposition and sequestration of organic carbon and nitrogen in fine soil fractions. *Biol. Fertil. Soils* **2015**, *51*, 427–442.
50. Hatton, P.-J.; Remusat, L.; Zeller, B.; Brewer, E.A.; Derrien, D. NanoSIMS investigation of glycine-derived C and N retention with soil organo-mineral associations. *Biogeochemistry* **2015**, *125*, 303–313.
51. Hatton, P.-J.; Bodé, S.; Angeli, N.; Boeckx, P.; Zeller, B.; Boiry, S.; Gelhaye, L.; Derrien, D. Assimilation and accumulation of C by fungi and bacteria attached to soil density fractions. *Soil Biol. Biochem.* **2014**, *79*, 132–139.
52. Baldock, J.; Nelson, P. Soil organic matter. In *Handbook of soil science*; Summer, M., Ed.; CRC Press: New York, USA, 1999; pp. B25–B84.
53. Chenu, C.; Plante, A. Clay-sized organo-mineral complexes in a cultivation chronosequence : revisiting the concept of the "primary organo-mineral complex." *Eur. J. Soil Sci.* **2006**, *57*, 596–607.
54. Battey, M. *Mineralogy for students*; Hafner Press: New York, 1972;
55. Barthelmy, D. Webmineral - Mineralogy database Available online: http://www.webmineral.com (accessed on Jul 10, 2018).

56. Deer, W.; Howie, R.; Zussman, J. *An introduction to the rock-forming minerals*; Longman: London, 1966;
57. Fischenner, R. *Données des principales espèces minérales*; Société de l'industrie minérale: St-Étienne (Loire), 1977;
58. Jouenne, C. *Céramique Générale - Notions de physico-chimie. Tome 1 (In French)*; Gauthier-Villars: Paris, 1960;
59. Mincryst Crystallographic and crystallochemical database for minerals and their structural analogues Available online: http://database.iem.ac.ru/mincryst (accessed on 10 July 2018).
60. Mindat Mineral and locality database Available online: http://www.mindat.org (accessed on 10 July 2018).

© 2020 by the authors. Licensee MDPI, Basel, Switzerland. This article is an open access article distributed under the terms and conditions of the Creative Commons Attribution (CC BY) license (http://creativecommons.org/licenses/by/4.0/).